

1      **Adoptive transfer of mitochondrial antigen-specific CD8<sup>+</sup> T-cells in mice causes parkinsonism and**  
2      **compromises the dopamine system.**

3  
4  
5  
6      Elemeery MN<sup>1-2-3-4-5-6-7</sup>, Tchung A<sup>1-2-3-4</sup>, Boulet S<sup>5-7</sup>, Mukherjee S<sup>1-2-3-4-5</sup>, Giguère N<sup>1-2-3-4-5</sup>, Daudelin J-  
7      F<sup>5-7</sup>, Even A<sup>1-2-3-4-5</sup>, Hétu-Arbour R<sup>5-7-8</sup>, Matheoud D<sup>2, 9</sup>, Stratton JA<sup>5,10</sup>, Labrecque N<sup>5-7-8-9-11-12\*</sup>,  
8      Trudeau L-E<sup>1-2-3-4-5\*</sup>

9  
10      \*Co-corresponding authors

11  
12      <sup>1</sup>Department of pharmacology and physiology, Faculty of Medicine, Université de Montréal

13      <sup>2</sup>Department of neurosciences, Faculty of Medicine, Université de Montréal

14      <sup>3</sup>Neural Signaling and Circuitry research group (SNC)

15      <sup>4</sup>Center for Interdisciplinary Research on the Brain and Learning (CIRCA)

16      <sup>5</sup>Aligning Science Across Parkinson's (ASAP) Collaborative Research Network, Chevy Chase, MD,  
17      USA, 20815.

18      <sup>6</sup>Medical Biotechnology Department, National Research Centre, Dokki, Giza, Egypt

19      <sup>7</sup>Centre de recherche de l'hôpital Maisonneuve-Rosemont (CRHMR)

20      <sup>8</sup>Institut de recherches cliniques de Montréal (IRCM)

21      <sup>9</sup>Centre de recherche du Centre hospitalier universitaire de l'Université de Montréal (CRCHUM)

22      <sup>10</sup>Dept. of Neuroscience and Neurology, Montreal Neurological Institute-Hospital, McGill University,  
23      Montreal,

24      <sup>11</sup>Department of medicine, Faculty of Medicine, Université de Montréal

25      <sup>12</sup>Department of microbiology, infectious diseases and immunology, Faculty of Medicine, Université de  
26      Montréal

27      **Running Title:** Mitochondrial peptide-specific T cells and Parkinson's disease.

28  
29      **Corresponding authors:**

30      Dr. Louis-Éric Trudeau

31      Department of pharmacology and physiology

32      Faculty of Medicine

33      Université de Montréal

34      louis-eric.trudeau@umontreal.ca

35      514-343-5692

36      Dr. Nathalie Labrecque

37      Institut de recherches cliniques de Montréal

38      Department of medicine

39      Faculty of medicine

40      Université de Montréal

41      nathalie.labrecque@umontreal.ca

42      514-987-5502

## Abstract

46

47

48 The progressive dysfunction and degeneration of dopamine (DA) neurons of the ventral midbrain is  
49 linked to the development of motor symptoms in Parkinson's disease (PD). Multiple lines of evidence  
50 suggest the implication of neuroinflammation and mitochondrial dysfunction as key drivers of  
51 neurodegenerative mechanisms in PD. Recent work has revealed that loss of the mitochondrial kinase  
52 PINK1 leads to enhanced mitochondrial antigen presentation (MitAP) by antigen-presenting cells  
53 (APCs), the amplification of mitochondrial antigen-specific CD8<sup>+</sup> T cells and the loss of DA neuron  
54 terminals markers in the brain in response to gut infection. However, whether mitochondrial antigen-  
55 specific T cells are involved in and/or sufficient to cause DA system dysfunction remains unclear. Here,  
56 we investigated the effect of mitochondrial autoimmunity by adoptively transferring mitochondrial  
57 peptide-specific CD8<sup>+</sup> T cells into wild-type (WT) and PINK1 KO mice. We find that this leads to L-  
58 DOPA-reversible motor impairment and to robust loss of DA neurons and axonal markers in the  
59 striatum in both PINK1 WT and KO mice. Our findings provide direct evidence of the pivotal role  
60 played by mitochondrial-specific CD8<sup>+</sup> T cell infiltration in the brain in driving PD-like pathology and  
61 the development of parkinsonism. Altogether, our data strongly support the hypothesis that MitAP and  
62 autoimmune mechanisms play a key role in the pathophysiological processes leading to PD.

63

64

**65 Key words:** Parkinson's, lymphocytes, dopamine, mitochondria, immune, PINK1

66

67

## Introduction

70 The motor symptoms of Parkinson's disease (PD), including bradykinesia, akinesia, rigidity and  
71 tremors, are caused in part by the progressive degeneration of substantia nigra pars compacta (SNc)  
72 dopamine (DA) neurons, leading to loss of DA in the striatum and dysregulation of basal ganglia circuits  
73 that regulate movement initiation. Disease modifying therapies are not presently available and current  
74 therapeutic strategies such as L-DOPA or DA receptor agonists focus on alleviating symptoms by  
75 partially restoring basal ganglia circuit function. A growing literature emerging from the study of the  
76 genes linked to familial, genetic forms of PD, suggests that the functions of ubiquitous cellular  
77 compartments such as mitochondria, lysosomes and vesicles are compromised by the loss of function of  
78 proteins such as PINK1 or Parkin [1-5] found in mitochondria or LRRK2 and GBA [6-9], found in  
79 lysosomes. Cellular dysfunctions could thus happen in multiple cell types and not only in neurons.

80 Cells of the immune system and inflammatory mechanisms are increasingly considered as  
81 playing a role in the initiation or progression of PD. Notably, increased levels of cytokines such as IL-  
82 1 $\beta$ , TNF- $\alpha$ , IFN- $\gamma$  and IL-6 have been reported in the cerebrospinal fluid and nigrostriatal regions of PD  
83 subjects relative to age-matched controls [10, 11]. The presence of T cells in the brain of PD subjects  
84 has also been reported [12] as well as the presence in the blood of antibodies and T cells recognizing  
85 alpha-synuclein antigens [13-15]. Entry of CD4 $^{+}$  T cells in the brain of a PD mouse model  
86 overexpressing alpha-synuclein has also been reported [16, 17], and increased brain inflammation and  
87 neuronal loss has been found in rats overexpressing alpha-synuclein [18]. Loss of function of PINK1 or  
88 Parkin was discovered to lead to disinhibition of mitochondrial antigen presentation (MitAP) in antigen  
89 presenting cells (APCs) [1]. Furthermore, in PINK1 KO mice, a gastrointestinal infection was shown to  
90 lead to the amplification of mitochondrial antigen-specific CD8 $^{+}$  T cells, to loss of DA neuron terminals

91 markers in the striatum and to impaired motor functions [19]. Together, this work raises the possibility  
92 that autoantigens and autoimmune mechanisms are involved in PD [20-22], a conclusion also supported  
93 by recent work on LRRK2 [23].

94 However, whether mitochondrial antigen-specific T cells are sufficient to cause DA system  
95 dysfunction remains undetermined and a critical question to tackle. To address this possibility, here we  
96 took advantage of 2C transgenic mice that express a T cell receptor (TCR) specific for a mitochondrial  
97 antigen derived from 2-oxoglutarate dehydrogenase (OGDH) [24, 25]. We tested the hypothesis that  
98 peripheral adoptive transfer of activated CD8<sup>+</sup> T cells from 2C mice in PINK1 KO mice would lead to  
99 an attack of the DA system in the brain of these mice. Compatible with this hypothesis, we find that this  
100 leads to L-DOPA reversible motor impairment and to robust loss of DA neurons and axonal markers in  
101 the striatum in both PINK1 WT and KO mice. This work establishes a new mouse model that could be  
102 critical to identify the mechanisms whereby mitochondrial antigen-specific CD8<sup>+</sup> T cells interact with  
103 DA neurons and other vulnerable neurons, leading to brain pathology in PD.

104  
105  
106 **Materials and methods**  
107

108 **Mice.** 2C[24, 25], OT-I[26] and Pink1 KO mice (Jackson Laboratory, Strain #017946) and wild type  
109 (WT) littermate controls were maintained in rigorous adherence to the principles of good animal practice  
110 as defined by the Canadian Council on Animal care and according to protocols approved by the animal  
111 ethics committee (CDEA) of the Université de Montréal and of the Research Center of the  
112 Maisonneuve-Rosemont Hospital.

114 **T cell purification and activation.** Naïve CD8<sup>+</sup> T cells from the spleen of 2C and OT-I TCR transgenic  
115 mice were purified using a Easysep<sup>TM</sup> Mouse naïve CD8<sup>+</sup> purification kit (STEMCELL, BC, Canada).  
116 Purified naïve CD8<sup>+</sup> T cells were then activated using anti-CD3/CD28 stimulation. Briefly, 24-wells  
117 plates were coated with 1 µg/ml of anti-CD3 antibody (BioXcell, clone 14-2C11; Cat # BE0001-1)  
118 diluted in sterile PBS and then incubated at 5% CO<sub>2</sub> at 37°C for 2h. 10<sup>6</sup> naïve CD8<sup>+</sup> T cells were seeded  
119 on CD3-coated wells and anti-CD28 antibody (BioXcell, clone 37-51; cat # BE0015-1) was added to  
120 reach a final concentration of 5 µg/ml. Cells were stimulated for 72h at 37°C before harvesting for  
121 adoptive transfer. The proper activation of CD8<sup>+</sup> T cells was validated by measuring the up-regulation of  
122 CD44, CD25 and CD69 and down-regulation of CD62L by flow cytometry.

123

124 **Adoptive transfer of TCR transgenic T cells.** Pink1 KO and WT littermate control mice were injected  
125 i.p with 5 X 10<sup>6</sup> activated 2C or OT-I CD8<sup>+</sup> T cells diluted in 200 µl of sterile PBS. Some control mice  
126 were not injected with T cells. 48h after adoptive transfer, all mice were treated with pertussis toxin  
127 (PTx) ( i.p 20ug/kg; Cayman chemical, cat# 23221) to facilitate T cell infiltration in the brain.

128

129 **FACS analysis.** 200 µl blood samples were collected in PBS containing 2mM EDTA from jugular vein  
130 at both early (day 7) and late (day 40) time points after the adoptive transfer. Spleens were also collected  
131 at day 7 for some mice and from all the mice at end point. Red blood cells were lysed using NH4CL  
132 0.86% before staining. Samples were stained first with the Zombie NIR viability dye (1:1,000) for 20  
133 min at 37°C, then with anti-CD16/CD32 for 20 min at 37°C followed by staining with antibodies  
134 directed against different cell surface markers for 20 min at 4°C. To track OT-I cells, K<sup>b</sup>-OVA tetramer  
135 (NIH Tetramer core facility) staining was done at 37°C for 15min. Samples were analyzed using the BD  
136 LSRFortessa X-20. The antibodies used for flow cytometry are listed in **Table 1**.

138 **Table 1: List of antibodies used for flow cytometry.**

<b>Antibody</b>		<b>Supplier</b>	<b>Product information</b>
<b>1B2</b>	Biotin	Custom made	F23.1, 53-6.72 (rat anti-mouse CD8).
<b>CD101</b>	PE-Cy7	ThermoFisher	Clone Moushi101; cat # 25-1011-80
<b>CD11b</b>	BV711	Biolegend	Clone M1/70; cat # 101242
<b>CD127</b>	BV421	Biolegend	Clone A7R34, cat # 135027
<b>CD25</b>	APC	Biolegend	Clone PC61; cat # 102012
<b>CD4</b>	BV605	Biolegend	Clone RM4-5; cat # 100548
<b>CD44</b>	APC-cy7	Biolegend	Clone IM7; cat # 103028
<b>CD45.2</b>	FITC	Biolegend	Clone 104; cat # 110706
<b>CD45.2</b>	Alexa flour 700	Biolegend	Clone 104; cat # 109822
<b>CD62L</b>	PercP	Biolegend	Clone MEL; cat # 104430
<b>CD69</b>	APC	Biolegend	Clone H1.2F3; cat # 104513
<b>CD8</b>	BV785	Biolegend	Clone 53-6.7; cat # 100750
<b>CXCR3</b>	PE	Biolegend	Clone CXCR3-173; cat # 126505
<b>CXCR6</b>	PEdazzle594	Biolegend	Clone SA051D1; cat # 151116
<b>KLRG1</b>	APC	Biolegend	Clone 1MAFA; cat # 138412
<b>P2XR7</b>	PercP-Cy5.5	Biolegend	Clone 1F11; cat # 148710
<b>K<sup>b</sup>-OVA<sub>257-264</sub></b>		NIH Tetramer core facility	

140 **Isolation of brain infiltrating lymphocytes.** To discriminate the T cells that have infiltrated the brain  
141 from the ones circulating in the blood, mice were injected i.v. with anti-CD45-FITC (BD) and sacrificed  
142 3-5 min later for brain collection. The T cells that have infiltrated the brain are protected from this short  
143 staining and as such, will be CD45-FITC negative in the flow cytometry analysis. To dissociate the  
144 brain, the tissue was minced using a scalpel longitudinally to not less than 8 pieces and digested in  
145 RPMI containing 0.01 mg/ml DNase I and 0.5 mg/ml collagenase D for 40 min using the gentleMACS  
146 Octo dissociator at 37°C before filtration through a 70µm filter. To isolate lymphocytes, samples were  
147 centrifuged, resuspended in 3 ml of 37% Percoll solution diluted in RPMI, layered over another 3 ml of  
148 70% Percoll, and centrifuged at 2000 r.p.m. without brake at 25 °C for 20min to collect the buffy coat  
149 leukocytes interlayer.

150

151 **Immunohistochemistry.** To prepare brain sections, PINK1 KO and WT littermate mice were deeply  
152 anaesthetized with pentobarbital (70 ug g<sup>-1</sup>, i.p.) before intracardiac perfusion with 50ml cold PBS (0.01  
153 M) followed by 50ml of cold 4% paraformaldehyde (PFA). Then, the brain was collected, post-fixed for  
154 24h in PFA solution at 4°C, followed 30% sucrose solution (5.382g/l sodium phosphate monobasic,  
155 8.662g/l sodium phosphate dibasic anhydrous, and 300g/l sucrose, dissolved in distilled water) for 48h.  
156 Serial coronal (40µm thickness) free-floating sections were cut using a Leica CM1950 cryostat and  
157 collected in an antifreeze solution (1.57g/l sodium phosphate monobasic anhydrous, 5.45g/l sodium  
158 phosphate dibasic anhydrous, 300ml ethylene glycol, 300ml glycerol, dissolved in distilled water).  
159 Coronal sections underwent permeabilization using Triton X-100 (0.1%), after which nonspecific  
160 binding sites were blocked by incubating in bovine serum albumin (100 mg/ml) (0.02% NaN3, 0.3%  
161 Triton X-100, 10% BSA, and 5% serum of the same host used for the secondary antibody). Sections  
162 then underwent permeabilization using a Triton X-100 (0.1%) based solution (0.02% NaN3, 0.1% Triton

163 X-100, 0.5% BSA, and 5% serum). The sections were subsequently incubated overnight with a rabbit  
164 anti-TH antibody (1:2000, AB152, Millipore Sigma, USA), a rat anti-DAT antibody (1:2000, MAB369;  
165 MilliporeSigma, USA), rabbit anti-Sert antibody (1:2000, PC177L-100UL, Sigma, USA) or mouse anti-  
166 NeuN antibody (1:1000, Abcam, USA) as well as DAPI to label nuclei (1:2000, D9542, Sigma Aldrich,  
167 USA). Quantitative analyses of fluorescence imaging on brain slices were conducted using images  
168 acquired through a Nikon AX-R automated point-scanning confocal microscope (Nikon NY, U.S.A).  
169 Images (2048x2048 px resolution, Nyquist, galvanometer scanning mode with 1x averaging and 0.8ms  
170 dwell time) were captured using PLAN APO AD 40 $\times$  OFN25 DIC N2 objective lens (0.6 NA, Nikon  
171 Canada) from dorsal and ventral striatum fields. The dorsal striatum encompassed the compartment  
172 superior to the anterior commissure and inferior to the corpus callosum, while the ventral striatum  
173 included the nucleus accumbens shell and core. In the dorsal striatum, image acquisition involved  
174 selecting four random fields on each side from both hemispheres in each section. In the ventral striatum,  
175 two fields per hemisphere were chosen in each section. Image quantification, performed using FIJI  
176 (National Institutes of Health) software, entailed applying a uniform threshold to all analyzed images  
177 after determining the average background signal intensity, which was then subtracted from the raw  
178 images. The quantification of TH+ and SERT+ axon terminals in dorsal striatal sections involved  
179 averaging eight fields per section, with eight independent sections quantified for each mouse. In the  
180 ventral striatum sections, the analysis averaged four fields per section, and five independent sections  
181 were quantified for each mouse.

182

183 **Stereological analysis.** Brain sections were rinsed in 0.01 M PBS for 10min before immersion in 0.01  
184 M PBS with 0.9% H<sub>2</sub>O<sub>2</sub> for another 10min. The sections were then rinsed three times in 0.01 M PBS  
185 after which they were incubated with rabbit anti-TH antibody at a 1:1000 dilution in a solution

186 containing 0.3% Triton X-100, 50 mg/ml BSA, and 0.01 M PBS, for 48h at 4°C. This was followed by  
187 further rinses in 0.01 M PBS (3 × 10min) and a 12h incubation at 4 °C in biotin-streptavidin conjugated  
188 AffiniPure IgG (anti-rabbit-streptavidin Jackson Immunoresearch, 1:200), followed by three washes  
189 with 0.01 M PBS. Subsequently, sections were incubated for 3h at room temperature in streptavidin  
190 horseradish peroxidase (HRP) conjugate (GE Healthcare, 1:200) diluted in 0.3% Triton X-100 in 0.01 M  
191 PBS. Visualization was achieved through a 5min 3,3'-diaminobenzidine tetrahydrochloride (Sigma-  
192 Aldrich)/glucose oxidase reaction, after which sections were mounted on charged microscope slides in  
193 0.1 M acetate buffer, counterstained with cresyl violet, defatted via a series of ethanol and xylene baths,  
194 and finally coverslipped using permount (Fisher Scientific. Cat # SP15-100). The quantification of the  
195 number of TH neurons in both the substantia nigra pars compacta (SNC) and ventral tegmental area  
196 (VTA) employed unbiased stereological counting methods. The total number of TH neurons was  
197 determined using the optical fractionator method [27] with Stereo Investigator (version 6;  
198 MicroBrightField). Briefly, TH-immunoreactive neurons were counted in every sixth section at 100×  
199 magnification using a 60 × 60- $\mu\text{m}^2$  counting frame. A 10 $\mu\text{m}$  optical dissector with two 1 $\mu\text{m}$  guard zones  
200 was utilized, and counting sites were positioned at 100 $\mu\text{m}$  intervals following a random start. A  
201 minimum number of 6 brain sections from each mouse including the SNC was used as an inclusion  
202 criterion.

203

204 **Behavioral tests.** All behavioral experiments were performed during the night cycle (active phase for  
205 mice), on both female and male mice of both genotypes. The investigator was blinded to both genotype  
206 and the treatment group during experimental procedures. To reduce the stress introduced by the  
207 examiner on the mice, mice were allowed to habituate to the examiner for not less than 5min per mice  
208 for 3 to 5 successive days. Mice housed at 2-4 mice in a cage were then tested at 42 to 52 days after the

209 adoptive transfer. On the test day, mice were transferred to the testing room and allowed a resting time  
210 of 60min before testing.

211

212 **Basal locomotor activity.** Open field automated activity chambers (Superflex, Omnitech, U.S.A) were  
213 used to quantify horizontal activity and vertical episode counts. All experiments were performed at the  
214 same time of the day using mice maintained on a 12h light/dark cycle from 22:00 to 10:00. Mice were  
215 placed individually in activity boxes (41 × 41 cm) and their horizontal and vertical activity were  
216 measured by quantifying photocell beam breaks. Data were analyzed by the fusion software version 5.3  
217 (Omnitech, Ohio, U.S.A).

218

219 **Grip strength test.** Grip strength tests were performed with a grip strength meter (BioSeb, France,  
220 model Bio-GS3). Mice were tested three times, and the results were averaged for each mouse. The  
221 muscular strength of mice was quantified by measuring the force needed (g) to remove the four paws  
222 from the grid. Each mouse was weighed before the grip strength test. Results are expressed as gram-  
223 force normalized to body weight.

224

225 **Pole test.** The pole utilized in this experiment was a 60cm metal rod with a diameter of 10mm. The rod  
226 was covered with adhesive tape to enhance traction and securely positioned within a housing cage. Mice  
227 were oriented head-up at the top of the pole, and the time taken for both turning and to complete descent  
228 was meticulously recorded. Treatment groups received either 6.5 mg/kg of benserazide (Sigma, B7283)  
229 combined with 25 mg/kg of l-DOPA (Sigma, D1507), or an equivalent volume of saline. Mice that did  
230 not descend from the pole after 180s were considered to have failed the test, returned to their home cage  
231 and re-tested later.

## Results

233  
234 **Mitochondrial peptide-specific CD8<sup>+</sup> T cells infiltrate the brain and are found in higher numbers**  
235 **in PINK1 KO mice.**

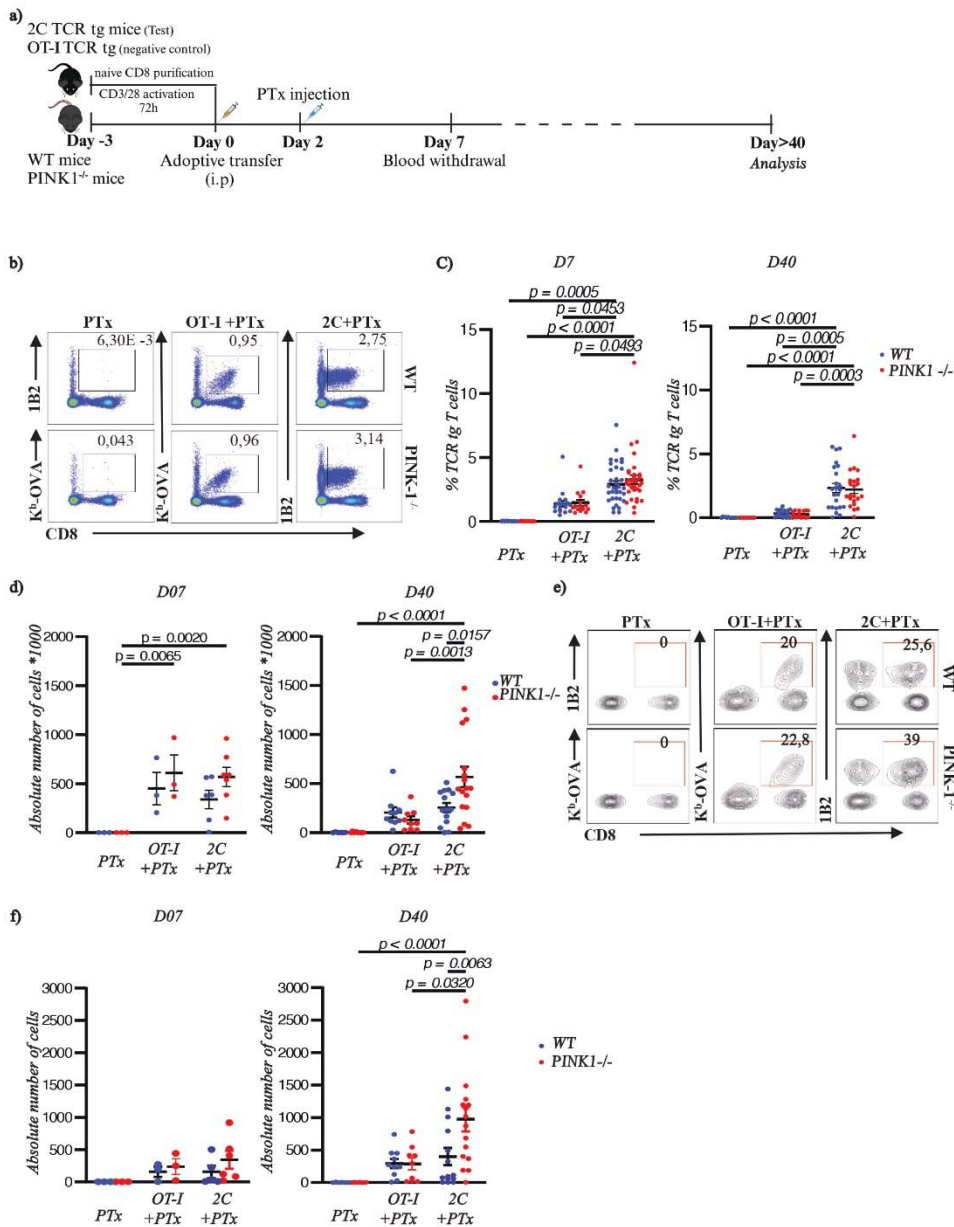
We tested the hypothesis that mitochondrial peptide-specific CD8<sup>+</sup> T-cells can induce PD-like pathology and parkinsonism in mice following their adoptive transfer into PINK1 KO mice. To do so, we adoptively transferred 5 X 10<sup>6</sup> *in vitro* activated CD8<sup>+</sup> T cells from 2C TCR transgenic mice, which express a TCR specific for the mitochondrial antigen OGDH, into PINK1 WT or KO mice (**Fig. 1a**). As a control, PINK1 WT and KO mice were adoptively transferred with activated CD8<sup>+</sup> T cells from OT-I TCR transgenic mice expressing a TCR specific for the ovalbumin antigen. Forty-eight hours after adoptive transfer, pertussis toxin (20 µg/kg) was administered i.p. to facilitate brain infiltration of the transferred CD8<sup>+</sup> T cells. Blood samples were collected at day 7 or 40 after the adoptive transfer to assess the persistence and abundance of the transferred cells. The transferred cells were tracked using either a monoclonal antibody (1B2) specific for the TCR expressed by the 2C CD8<sup>+</sup> T cells or with the K<sup>b</sup>-OVA tetramer for control OT-I CD8<sup>+</sup> T cells. The gating strategy is described in **Supplemental Fig. 1**. We were able to detect the transferred 2C and OT-I CD8<sup>+</sup> T cells in the blood of the recipient mice both at 7 and 40 days after the adoptive transfer, with a higher frequency of the 2C compared to the OT-I CD8<sup>+</sup> T cells (**Fig. 1b-c**). Although the proportion of 2C CD8<sup>+</sup> T cells in the blood of the transferred mice was not significantly different between PINK1 KO and WT mice (**Fig. 1b-c**), the absolute number of such cells detected in the spleen at day 40 was higher in the PINK1 KO mice compared to WT littermates (**Fig. 1d and Supplementary Fig.1**). Altogether, these observations indicate that mitochondrial peptide-specific 2C CD8<sup>+</sup> T-cells accumulate more than OT-I CD8<sup>+</sup> T cells in PINK1 KO and WT mice suggesting that 2C T cells encounter their antigen in recipient mice. Moreover, as more

255 2C CD8<sup>+</sup> T cells were recovered in PINK1 KO mice compared to PINK1 WT recipients, these findings  
256 suggest that they may have seen more mitochondrial antigens in PINK1 KO mice.

257 We then asked whether the adoptively transferred 2C CD8<sup>+</sup> T cells were infiltrating the brain of  
258 the recipient mice. Seven or 40 days after the adoptive T cell transfer, FITC-labelled anti-CD45  
259 antibodies were injected i.v. 3-5 min prior to brain collection. This allows to label circulating  
260 lymphocytes and distinguish them from those that had entered in the brain (**Supplementary Fig. 1**). We  
261 found that both 2C and OT-I CD8<sup>+</sup> T cells infiltrated the brain and were readily detectable at both 7 and  
262 40 days after the adoptive transfer, with an increased abundance at day 40 (**Fig. 1e-f**). The absolute  
263 number of 2C CD8<sup>+</sup> T cells was higher in PINK1 KO mice compared to WT control mice (**Fig. 1e-f**).  
264 The results demonstrate that mitochondrial antigen-specific CD8<sup>+</sup> T-cells infiltrate and accumulate in  
265 the brain, and this is enhanced in the absence of functional PINK1 protein in the recipient mice.

266

Figure 1



267

268 **Figure 1: Adoptively transferred mitochondrial antigen-specific CD8<sup>+</sup> T cells persist in the circulation and infiltrate**  
269 **the brain in higher amounts in PINK1 KO mice. a)** Schematic diagram outlining the experimental workflow. **b)**  
270 Representative flow cytometry profiles for the detection of adoptively transfer TCR transgenic CD8<sup>+</sup> T cells. 2C T cells were  
271 identified using the anti-TCR clonotype antibody 1B2 (CD8+1B2+) while OT-I T cells were identified using K<sup>b</sup>-OVA  
272 tetramer staining (CD8+K<sup>b</sup>-OVA+). PTx refers to mice that were not adoptively transferred and only received the Ptx  
273 treatment. **c)** Frequency of the adoptively transferred TCR transgenic CD8<sup>+</sup> T cells in the blood at day 7 and 40 after the  
274 adoptive transfer in WT and PINK1 KO mice. **d)** Absolute number of adoptively transferred TCR transgenic CD8<sup>+</sup> T cells in  
275 the spleen of WT and PINK1 KO mice. **e)** Representative flow cytometry profiles for the detection of adoptively transfer  
276 TCR transgenic CD8<sup>+</sup> T cells that have infiltrated into the brain. **f)** Absolute number of adoptively transferred TCR  
277 transgenic CD8<sup>+</sup> T cells that infiltrated the brain of WT and PINK1 KO mice at 7 days (left) and 40 days (right) after the

278 adoptive transfer. Each dot represents the results obtained from one mouse. Data is representative of a minimum of three  
279 independent experiments. p values were determined using two-way ANOVA followed by Tukey's multiple comparisons  
280 post-hoc test. Data are presented as mean  $\pm$  s.e.m. Data from male and female mice were pooled.

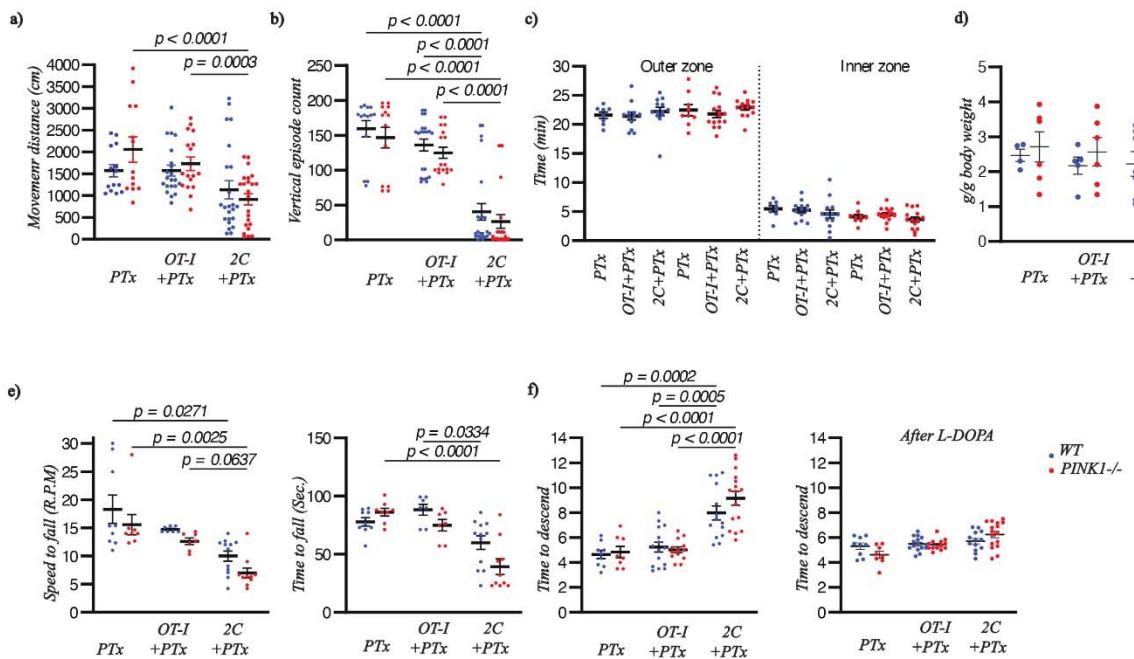
281

282 **Adoptive transfer of mitochondrial antigen-specific CD8<sup>+</sup> T cells leads to L-DOPA reversible**  
283 **motor impairment in both PINK1 KO and WT mice.**

284 Our observation of entry of the adoptively transferred CD8<sup>+</sup> T cells in the brain raised the possibility  
285 that mitochondrial antigen-specific 2C CD8<sup>+</sup> T cells could recognize their antigen in the brain, leading  
286 to DA neuron loss and motor circuit dysfunction. Compatible with this hypothesis, we observed that  
287 after a period of 30 days or more following the adoptive transfer, some of the mice showed impaired  
288 locomotion in their home cages following qualitative observations. To validate this, we performed more  
289 extensive behavioral phenotyping using open field locomotor analysis, grip strength analysis, a rotarod  
290 task and the pole test. In the open field, we found reduced movement distance and vertical episodes in  
291 the mice transferred with 2C CD8<sup>+</sup> T cells, but not in the mice transferred with OT-I CD8<sup>+</sup> T cells or  
292 only injected with Ptx (Fig. 2a-b). Similar effects were seen in PINK1 KO and WT recipients. The time  
293 spent in the center of the open field, often used as an indirect index of anxiety, was not altered (Fig. 2c).  
294 No differences were observed in the grip strength test (Fig. 2d). In the rotarod task, the maximal speed  
295 leading to falling off the apparatus and the time to fall was lower in the mice that had undergone 2C  
296 CD8<sup>+</sup> T cell adoptive transfer compared to the other groups (Fig. 2e), with here again the genotype of  
297 the recipient mice having no impact. Finally, in the pole test, the mice transferred with 2C CD8<sup>+</sup> T cells,  
298 but not the mice transferred with OT-I CD8<sup>+</sup> T cells or treated only with PTx showed impaired  
299 performance, as revealed by a slower time to descend (Fig. 2f, left panel). This difference was not  
300 observed when mice were pre-treated with the DA synthesis precursor L-DOPA (Fig. 2f, right panel),  
301 arguing that the motor impairments observed in the adoptively transferred mice were linked to reduced

302 DA levels. Like for the other behavioral tests, PINK1 KO and WT littermates did not differ, suggesting  
 303 that a similar neurodegenerative process occurred in both genotypes.

Figure 2



304

305 **Figure 2: Adoptive transfer of mitochondrial antigen-specific CD8<sup>+</sup> T cells leads to L-DOPA reversible motor**  
 306 **impairment in both PINK1 KO and WT mice.** **a)** In the open field test, the mice were examined for a period of 30min.  
 307 Total movement distance travelled by mice in an open field arena was measured. **b)** Vertical episodes (number of time that  
 308 the mouse rears). **c)** Time spent in the outer zone vs inner zone of the open field. **d)** Grip strength for the four limbs  
 309 normalized by mouse body weight. **e)** Rotarod analysis of the maximal speed and time to fall. **f)** Time to descent in the  
 310 pole test before (left panel) and 15-30 min after i.p. administration of L-DOPA (25mg/kg) and the dopadecarboxylase  
 311 inhibitor benserazide (6.5 mg/kg) (right panel). Motor functions were analyzed between days 42 and 56 after the adoptive T  
 312 cell transfer. Data are representative of four independent experiments for a, b, c, and f and three independent experiments  
 313 for d and e. *p* values were determined via two-way ANOVA followed by Tukey's multiple comparison's test. Data are  
 314 presented as mean ± s.e.m. The data combines both male and female mice.

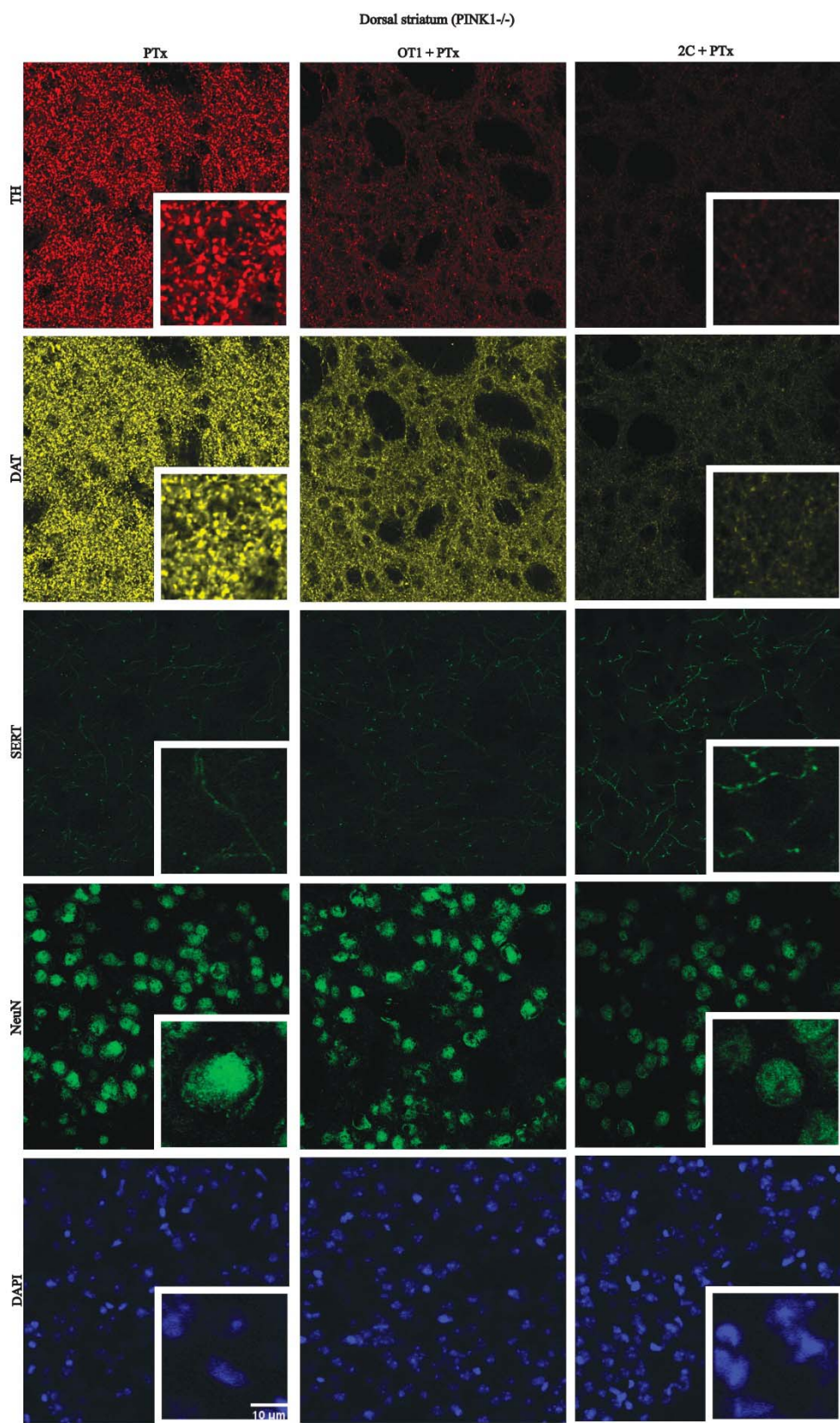
315

316 **Adoptive transfer of mitochondrial antigen-specific CD8<sup>+</sup> T cells causes dopaminergic denervation**  
 317 **in the striatum of both PINK1 KO and WT mice.**

318 The motor dysfunctions observed after adoptive transfer of 2C CD8<sup>+</sup> T cells could result from  
 319 perturbations of basal ganglia circuitry, leading to impaired motor commands. Because DA is a critical  
 320 regulator of basal ganglia circuitry and DA neurons are known to be particularly vulnerable to cellular  
 321 stress[28], we hypothesized that this system could be negatively affected by mechanisms driven by 2C

322 CD8<sup>+</sup> T cells entry in the brain. This hypothesis is also supported by prior *in vitro* work suggesting the  
323 capacity of DA neurons to express MHC class I molecules and present antigens to CD8<sup>+</sup> T cells[19, 29].  
324 Here, we used immunohistochemistry on brain sections prepared from mice 40 days after the adoptive  
325 transfer of CD8<sup>+</sup> T cells. We find that the dorsal striatum, the main projection area of SNc DA neurons  
326 and known to be most affected in PD, of mice that received 2C CD8<sup>+</sup> T cells showed a substantial loss  
327 of the density of both tyrosine hydroxylase (TH) and DA transporter (DAT) immunoreactivity (**Fig. 3**  
328 and **Fig. 4**). No significant changes were observed in mice adoptively transferred with OT-I CD8<sup>+</sup> T  
329 cells or in mice with only PTx treatment. In the ventral striatum, the same tendency was observed (**Fig.**  
330 **4** and **Supplementary Fig. 2**). Decreases in TH and DAT were similar in PINK1 KO and WT mice  
331 (**Fig. 4**). We also examined whether this loss of DA neuron axon terminal markers was selective or  
332 whether it affected other axonal projections to the striatum or neurons intrinsic to the striatum. For this,  
333 we quantified the levels of immunoreactivity for the serotonin (5-HT) axon terminal marker SERT (5-  
334 HT transporter) and NeuN, labelling all striatal neuron cell bodies. We found that these signals were not  
335 significantly changed (**Figs. 3-4 and Supplementary Fig. 2**). These observations are consistent with the  
336 hypothesis that the motor dysfunctions induced by the adoptive transfer of mitochondrial antigen-  
337 specific CD8<sup>+</sup> T cells and entry of these cells in the brain led to an attack on the DA system.

Figure 3

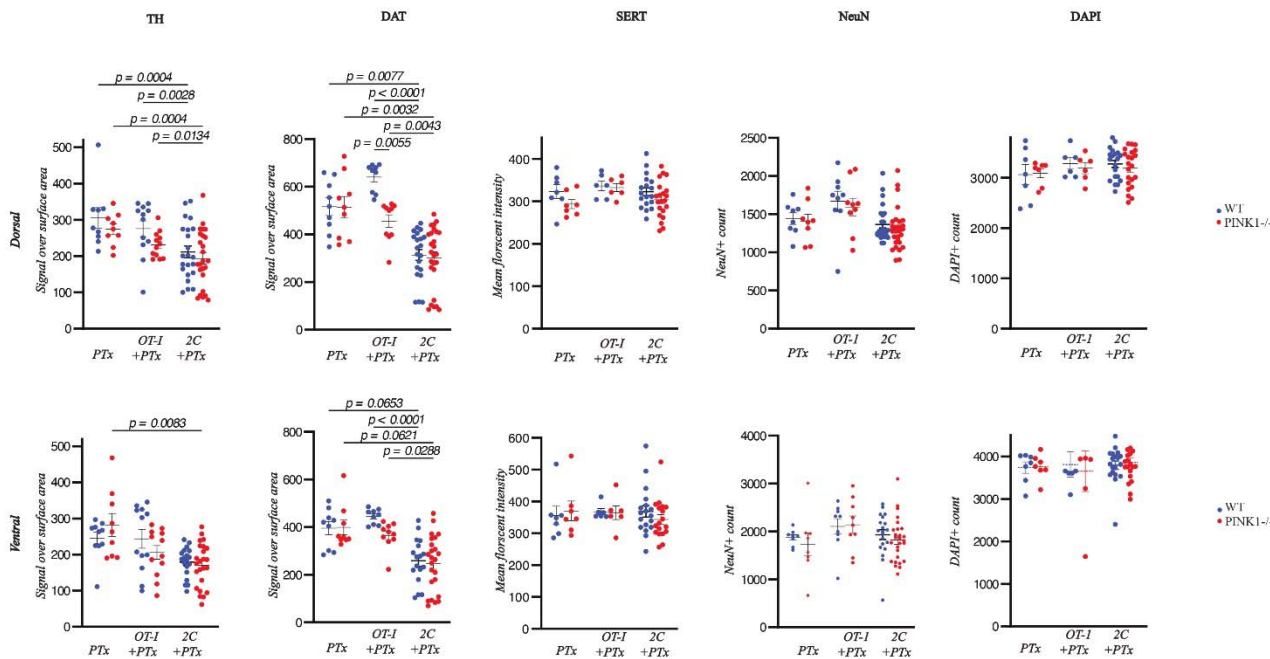


339  
340  
341  
342  
343  
344

**Figure 3 : Adoptive transfer of mitochondrial antigen-specific CD8<sup>+</sup> T cells causes dopaminergic denervation in the striatum of both PINK1 KO and WT mice.** Immunofluorescence staining of the dorsal striatum showing the expression of the dopaminergic neuronal markers tyrosine hydroxylase (TH) (red) and dopamine transporter (DAT) (yellow). The third row of images shows signal for the serotonin (5-HT) membrane transporter (SERT) (dark green). Finally, neuronal nuclei were localized with NeuN (bright green), while total cell population in the tissue was quantified using the nuclear stain DAPI (blue).

345

Figure 4



346

347  
348  
349  
350  
351  
352  
353

**Figure 4: Quantification of the changes in dopaminergic terminal markers reveals that adoptive transfer of mitochondrial antigen-specific CD8<sup>+</sup> T cells caused selective dopaminergic denervation in the striatum of both PINK1 KO and WT mice.** Quantification of TH, DAT, SERT signal intensity in the dorsal and ventral striatum as determined by signal strength per unit area. NeuN and DAPI represented as absolute count per unit area. Brains were collected at days 42-56 after the adoptive transfer of CD8<sup>+</sup> T cells. p value determined using two-way ANOVA, followed by Tukey's multiple comparison's test. Data are presented as mean  $\pm$  s.e.m.

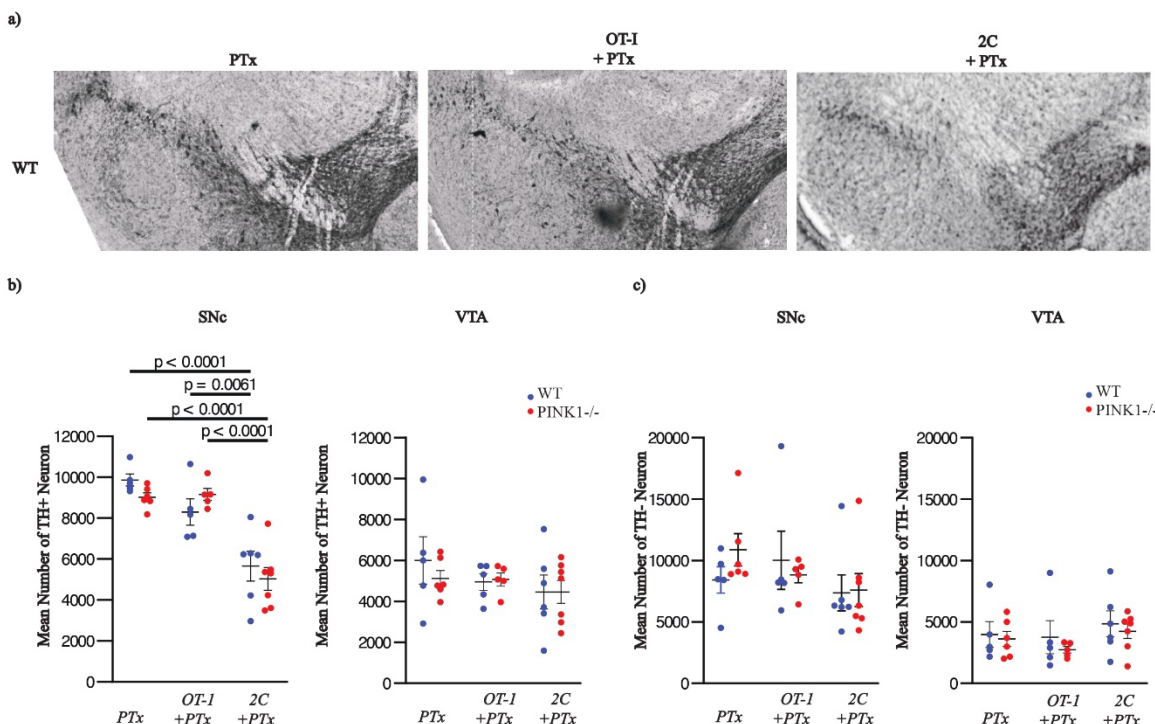
353

354 **Adoptive transfer of activated mitochondrial antigen-specific CD8<sup>+</sup> T cells leads to degeneration of**  
355 **dopamine neuron cell bodies in the substantia nigra**

356 Loss of axon terminal markers in the striatum could result from a selective attack on axon terminals or  
357 from loss of DA neuron cell bodies in the ventral midbrain, including the SNC and VTA. To examine  
358 this, we performed a separate series of immunohistochemistry quantification of TH immunoreactive cell  
359 bodies in the SNC and VTA using unbiased stereological counting methods. We found that the number

360 of DA neuron cell bodies was reduced in the SNc but not in the VTA following the adoptive transfer of  
 361 mitochondrial antigen-specific 2C CD8<sup>+</sup> T cells. This was not observed following transfer of the control  
 362 OT-I CD8<sup>+</sup> T cells (**Fig. 5a-b**). The extent of cell body loss was similar for PINK1 KO and WT mice  
 363 (**Fig. 5b**). Furthermore, no changes in the number of TH-negative neurons were observed (**Fig. 5c**).  
 364 Altogether, these observations suggest that the loss of terminal markers in the striatum induced by the  
 365 adoptive transfer of mitochondrial antigen-specific CD8<sup>+</sup> T cells is linked to the selective loss of SNc  
 366 DA neurons in the ventral midbrain.

Figure 5



367

368 **Figure 5: Adoptive transfer of activated mitochondrial antigen-specific CD8<sup>+</sup> T cells leads to loss of dopamine**  
 369 **neuron cell bodies in the substantia nigra.** a) Representative images of the DAB staining used for stereological counting  
 370 of TH+ dopaminergic neurons in the ventral midbrain. b-c) Stereological counting of TH+ and TH- neurons in the ventral  
 371 tegmental area (VTA) and substantia nigra pars compacta (SNc). Data pooled from three independent experiments. Data are  
 372 presented as mean  $\pm$  s.e.m.

373

374

375

376

## Discussion

379 The mechanisms leading in PD to the loss of DA neurons and other vulnerable neuronal subgroups such  
380 as noradrenergic neurons of the locus coeruleus are still ill-defined [28]. However, an increasing amount  
381 of evidence suggests that inflammation and immune mechanisms may be involved. A growing series of  
382 studies focusing on gene products linked to familial, genetic forms of PD, suggest that multiple PD-  
383 related proteins including Parkin, PINK1 and LRRK2 act as regulators of innate and adaptive immune  
384 responses in APCs and that loss of function of some of these proteins can amplify immune responses [1,  
385 13-15, 20-23, 30, 31]. Recent work showed that, in inflammatory conditions, PINK1 and Parkin play a  
386 role in restricting the presentation on MHC class I molecules of antigens derived from proteins present  
387 in the matrix of mitochondria. Indeed, the loss of expression of PINK1 increased MitAP while  
388 overexpression of Parkin inhibited this presentation pathway in response to the Gram-negative surface  
389 molecule lipopolysaccharide (LPS) in APCs *in vitro* [1]. These data led to the hypothesis that a loss of  
390 function of either PINK1 or Parkin results in the presentation of mitochondrial antigens and the  
391 stimulation of autoreactive CD8<sup>+</sup> T cells that contribute to the pathophysiological process leading to  
392 neuronal loss in PD. We have shown that MitAP can be activated following gut infection with Gram-  
393 negative bacteria in PINK1 KO mice, a process that leads to the activation of mitochondrial antigen-  
394 specific CD8<sup>+</sup> T cells and the concomitant development of motor impairments reversible by L-DOPA  
395 [19]. Although this chain of events was observed in infected PINK1 KO mice, evidence of a direct role  
396 for CD8<sup>+</sup> T cells in neuronal loss and the emergence of the motor impairments was not clearly  
397 established. Here we extend these previous observations by providing for the most direct test to date of  
398 the capacity of mitochondrial antigen-specific activated CD8<sup>+</sup> T cells to attack the DA system and cause  
399 parkinsonism in mice. Globally, our findings of brain entry and amplification of such CD8<sup>+</sup> T cells, loss

400 of DA neuron axon terminal markers in the striatum, loss of DA neuron cell bodies in the SNc and  
401 impaired motor functions support the hypothesis that entry of activated mitochondrial antigen-specific  
402 CD8<sup>+</sup> T cells in the brain is sufficient to cause neuronal damage and functional impairment.

403

404 We found that after adoptive transfer of *in vitro* activated CD8<sup>+</sup> T cells specific for either OGDH or  
405 ovalbumin, such cells are readily detectable in the periphery and brain of both PINK1 KO and WT mice.  
406 However, the abundance of mitochondrial antigen-specific 2C CD8<sup>+</sup>T cells in recipient mice 40 days  
407 after the transfer was higher compared to mice adoptively transferred with ovalbumin-specific CD8<sup>+</sup> T  
408 cells. This suggests that re-encountering of the antigen by 2C T cells promotes their accumulation and  
409 further indicates that the mitochondrial protein OGDH is being presented by MHC class I molecules *in*  
410 *vivo* at steady state in both the presence and absence of PINK1. This contrasts with previous work  
411 reporting an enhancement of mitochondrial antigen-presentation only in PINK1 KO mice [19]. This  
412 could perhaps result from the fact that previously activated CD8<sup>+</sup> T cells have a lower threshold for  
413 activation following antigen recognition. Although 2C T cells accumulate more than OT-I T cells, we  
414 found increased presence of 2C T cells in the spleen and the brain of PINK KO compared to PINK WT  
415 mice. These observations are compatible with the hypothesis that PINK1 deficiency leads to enhanced  
416 presentation of mitochondrial antigens as reported previously [1]. Alternatively, PINK1 deficiency could  
417 impact other aspects of the CD8<sup>+</sup> T cell response such as the cytokine milieu or functions of antigen-  
418 presenting cells.

419

420 Qualitative examination of the mice after the adoptive T cell transfer suggested the gradual appearance  
421 of motor dysfunctions. A more quantitative examination of the mice with a battery of behavioral tasks  
422 42-56 days after the adoptive transfer of CD8<sup>+</sup> T cells confirmed the presence of behavioral

423 impairments, both in the open field, rotarod and in the pole tests. Furthermore, the motor impairments in  
424 the pole test were reversed by L-DOPA administration, arguing in favor of the fact that they were caused  
425 at least in part by reduced DA levels in the brain. These observations are similar to what was previously  
426 observed in PINK1 KO mice after gastrointestinal infection in a previous study [19]. These findings  
427 extend the previous study by showing that CD8<sup>+</sup> T cells are likely to be a major driver of brain  
428 pathology and the appearance of parkinsonism. Further work will be required to determine whether  
429 other behaviors linked to non-motor symptoms of PD are also affected in these mice. This could include  
430 olfaction, sleep, gastrointestinal functions and cognition.

431

432 A surprising finding was that motor impairments developed both in PINK1 WT and KO mice upon T  
433 cell adoptive transfer. The fact that PINK1 inhibits the presentation of mitochondrial antigens by APCs  
434 suggests that one of the main roles of this protein in the context of PD is to prevent the initiation of the  
435 disease process by restricting the stimulation of auto-reactive CD8<sup>+</sup> T cells. Accordingly, introducing  
436 cytotoxic T cells by adoptive transfer would bypass the protective function of PINK1 and engage a  
437 pathophysiological process in both WT and KO mice. This implies that the presence of functional  
438 PINK1 proteins in DA neurons cannot prevent the damage to the dopaminergic system and the resulting  
439 motor impairments once cytotoxic T cells are elicited.

440

441 Our observation of a reduced density of DA neuron axon terminal markers in the striatum of the 2C but  
442 not in the OT-I CD8<sup>+</sup> T cells transferred mice provides a possible explanation for the L-DOPA-sensitive  
443 behavioral impairment observed in the present experiments. Our finding of a lack of change in 5-HT  
444 neuron axon terminal marker (SERT) in the same striatal sections argues that the T cell-mediated attack  
445 was not non-selective and had a larger impact on the brain's most vulnerable neurons. Our finding of

446 unaltered number of NeuN-positive neurons or total DAPI-positive cells in these striatal sections also  
447 suggests a lack of non-specific neuronal toxicity in these mice. Nonetheless, further examination of  
448 markers for other neurotransmitter systems possibly also affected in PD, such as norepinephrine and  
449 cholinergic neuromodulatory systems would help extend this conclusion.

450

451 The specific mechanisms at play, linking CD8<sup>+</sup> T cells entry and DA system dysfunction, remain to be  
452 examined. Based on previous work suggesting that DA neurons have the capacity to express MHC class  
453 I molecules on their surface [29], one possibility is that in these mice, following the adoptive transfer of  
454 2C CD8<sup>+</sup> T cells and PTx treatment, DA neurons present mitochondrial antigens leading to their direct  
455 recognition and attack by CD8<sup>+</sup> T cells. However, more work is needed to characterize the extent and  
456 dynamics of MHC class I expression by DA neurons in both PINK1 KO and WT mice. Our finding of  
457 an equivalent attack of DA neurons by activated 2C CD8<sup>+</sup> T cells in PINK1 KO and WT mice suggests  
458 that such antigen presentation could happen in both genotypes, although not necessarily at the same  
459 levels. This raises the hypothesis that in forms of PD linked to loss of PINK1 function, a critical step  
460 depends on peripheral mechanisms leading to the amplification of mitochondrial antigen-specific CD8<sup>+</sup>  
461 T cells. As such, the loss of PINK1 function directly in DA neurons may be less critical. Further work  
462 will be required to clarify this. Other than a direct attack of DA neurons by activated CD8<sup>+</sup> T cells,  
463 another possible mechanism could implicate MitAP by microglia, leading to the secretion of neurotoxic  
464 agents by both activated microglia and activated CD8<sup>+</sup> T cells. Such mechanisms could rely for example  
465 on the secretion of cytokines by CD8<sup>+</sup> T cells following recognition of their antigen on microglia,  
466 leading to activation of microglia that would then produce inflammatory mediators leading to DA  
467 neuron loss. Another possibility is that activated microglia produces ROS that selectively affects the DA

468 system. A growing literature suggests the implication of similar mechanisms implicating CD8 T cells in  
469 Alzheimer's disease [33-36].

470

471 Our work provides a different perspective on how PINK1 loss of function could lead to the dysfunction  
472 and loss of DA neurons. PINK1 was first shown to be involved in the clearance of damaged  
473 mitochondria by mitophagy [33, 37-40]. Such observations were taken by some to imply that loss of  
474 PINK1 function in DA neurons would lead to the accumulation of damaged mitochondria in these  
475 neurons, eventually promoting their death. However, mitophagy still proceeds in the absence of PINK1  
476 [41-44] and there is presently very limited evidence that dysfunctional mitochondria indeed accumulate  
477 in PINK1 or Parkin KO DA neurons [45]. Although we did not directly evaluate the functions of  
478 neuronal PINK1 in the present study, our results are more compatible with the hypothesis that loss of  
479 function of PINK1 engages autoimmune mechanisms in the periphery at early stages of the disease  
480 process. By disinhibiting MitAP and the activation of mitochondria antigen-specific CD8<sup>+</sup> T cells,  
481 shown here to be responsible for alteration of the dopaminergic system, loss of function of PINK1 may  
482 lead to enhanced activation of the immune system in what is likely to be a complex non-cell autonomous  
483 process responsible for DA neuron cell death and hallmark motor impairments.

484

485 Taken together, our observations provide unprecedented support for a key role of mitochondrial antigen-  
486 specific CD8<sup>+</sup> T cells in DA system perturbations and associated parkinsonism in mouse models of  
487 early-onset PD. This work could be instrumental for the development of better animal models of PD and  
488 for the identification of new immune-based therapeutic approaches to treat PD patients.

489

490

491 **Acknowledgements**

492 We would like to thank Drs. Michel Desjardins, Samantha Gruenheid, Heidi McBride and Janelle  
493 Drouin-Ouellet for their critical feedback during the development of this project. We also thank Dr.  
494 Numa Dancause for providing access to their stereological counting microscope system. The present  
495 study was funded by the joint efforts of the Michael J. Fox Foundation for Parkinson's Research (MJFF)  
496 and the Aligning Science Across Parkinson's (ASAP) initiative. MJFF administers the grant ASAP  
497 000525 on behalf of ASAP and itself. The Trudeau lab also received support from the Canadian  
498 Institutes of Health Research (CIHR) (grant 165928) and from the Krebil foundation. M. N. E.  
499 received a graduate student award from the mission sector of the ministry of higher education, Egypt.

500

501 **Author contributions**

502  
503 Conceptualization: N.L., D.M. and L-E.T.  
504 Methodology: M.N.E., J-F.D., A.T., S.B., S.M., N.G., R.H-A, A.E.  
505 Investigation: M.N.E., J-F.D., A.T., S.B., S.M., N.G., R.H-A, A.E.  
506 Supervision: N.L., J.A.S. and L-E.T.  
507 Writing—original draft: M.N.E., N.L. and L-E.T.  
508 Writing—review & editing: M.N.E., N.L. and L-E.T.

509

510 **Competing interests:**

511 The authors declare that they have no conflicts of interest.

512 **Data and materials availability:**

513 All key data is included in the manuscript. Access to original raw images is available on request from  
514 the corresponding authors.

515

516 **References**

517

518 1. Matheoud, D., et al., *Parkinson's disease-related proteins PINK1 and Parkin repress*  
519 *mitochondrial antigen presentation*. *Cell*, 2016. **166**(2): p. 314-327.

520 2. Drouin-Ouellet, J., et al., *Age-related pathological impairments in directly reprogrammed*  
521 *dopaminergic neurons derived from patients with idiopathic Parkinson's disease*. *Stem Cell*  
522 *Reports*, 2022. **17**(10): p. 2203-2219.

523 3. Drouin-Ouellet, J., *Mitochondrial complex I deficiency and Parkinson disease*. *Nat Rev*  
524 *Neurosci*, 2023. **24**(4): p. 193.

525 4. Fava, V.M., et al., *Pleiotropic effects for Parkin and LRRK2 in leprosy type-1 reactions and*  
526 *Parkinson's disease*. *Proc Natl Acad Sci U S A*, 2019. **116**(31): p. 15616-15624.

527 5. de Leseleuc, L., et al., *PARK2 mediates interleukin 6 and monocyte chemoattractant protein 1*  
528 *production by human macrophages*. *PLoS Negl Trop Dis*, 2013. **7**(1): p. e2015.

529 6. Wallings, R.L., et al., *ASO-mediated knockdown or kinase inhibition of G2019S-Lrrk2 modulates*  
530 *lysosomal tubule-associated antigen presentation in macrophages*. *Mol Ther Nucleic Acids*,  
531 2023. **34**: p. 102064.

532 7. Al-Azzawi, Z.A.M., S. Arfaie, and Z. Gan-Or, *GBA1 and The Immune System: A Potential Role*  
533 *in Parkinson's Disease?* *J Parkinsons Dis*, 2022. **12**(s1): p. S53-S64.

534 8. Kim, K.S., et al., *Regulation of myeloid cell phagocytosis by LRRK2 via WAVE2 complex*  
535 *stabilization is altered in Parkinson's disease*. *Proc Natl Acad Sci U S A*, 2018. **115**(22): p.  
536 E5164-E5173.

537 9. Taylor, M. and D.R. Alessi, *Advances in elucidating the function of leucine-rich repeat protein*  
538 *kinase-2 in normal cells and Parkinson's disease*. *Curr Opin Cell Biol*, 2020. **63**: p. 102-113.

539 10. Mount, M.P., et al., *Involvement of interferon- $\gamma$  in microglial-mediated loss of dopaminergic*  
540 *neurons*. *Journal of Neuroscience*, 2007. **27**(12): p. 3328-3337.

541 11. Koziorowski, D., et al., *Inflammatory cytokines and NT-proCNP in Parkinson's disease patients*.  
542 *Cytokine*, 2012. **60**(3): p. 762-766.

543 12. Brochard, V., et al., *scher, J. Callebert, J. Launay, C. Duyckaerts, RA Flavell, EC Hirsch and S.*  
544 *Hunot*. *The Journal of Clinical Investigation*, 2009. **119**: p. 182-192.

545 13. Singhania, A., et al., *The TCR repertoire of alpha-synuclein-specific T cells in Parkinson's*  
546 *disease is surprisingly diverse*. *Sci Rep*, 2021. **11**(1): p. 302.

547 14. Lindestam Arlehamn, C.S., et al., *alpha-Synuclein-specific T cell reactivity is associated with*  
548 *preclinical and early Parkinson's disease*. *Nat Commun*, 2020. **11**(1): p. 1875.

549 15. Sulzer, D., et al., *T cells from patients with Parkinson's disease recognize alpha-synuclein*  
550 *peptides*. *Nature*, 2017. **546**(7660): p. 656-661.

551 16. Schonhoff, A.M., et al., *Border-associated macrophages mediate the neuroinflammatory*  
552 *response in an alpha-synuclein model of Parkinson disease*. *Nat Commun*, 2023. **14**(1): p. 3754.

553 17. Williams, G.P., et al., *CD4 T cells mediate brain inflammation and neurodegeneration in a*  
554 *mouse model of Parkinson's disease*. *Brain*, 2021. **144**(7): p. 2047-2059.

555 18. Tiberi, M., et al., *Systemic inflammation triggers long-lasting neuroinflammation and*  
556 *accelerates neurodegeneration in a rat model of Parkinson's disease overexpressing human*  
557 *alpha-synuclein*. 2024.

558 19. Matheoud, D., et al., *Intestinal infection triggers Parkinson's disease-like symptoms in Pink1(-/-)*  
559 *mice*. *Nature*, 2019. **571**(7766): p. 565-569.

560 20. Hobson, B.D. and D. Sulzer, *Neuronal Presentation of Antigen and Its Possible Role in*  
561 *Parkinson's Disease*. *J Parkinsons Dis*, 2022. **12**(s1): p. S137-S147.

562 21. Garretti, F., et al., *T cells, alpha-synuclein and Parkinson disease*. Handb Clin Neurol, 2022.  
563 **184**: p. 439-455.

564 22. Fahmy, A.M., et al., *Mitochondrial antigen presentation: a mechanism linking Parkinson's*  
565 *disease to autoimmunity*. Curr Opin Immunol, 2019. **58**: p. 31-37.

566 23. Fahmy, A.M., et al., *LRRK2 regulates the activation of the unfolded protein response and*  
567 *antigen presentation in macrophages during inflammation*. bioRxiv, 2023: p. 2023.06.  
568 14.545012.

569 24. Sha, W.C., et al., *Selective expression of an antigen receptor on CD8-bearing T lymphocytes in*  
570 *transgenic mice*. Nature, 1988. **335**(6187): p. 271-274.

571 25. Ueda, K., et al., *Self-MHC-restricted peptides recognized by an alloreactive T lymphocyte*  
572 *clone*. Journal of Immunology (Baltimore, Md.: 1950), 1996. **157**(2): p. 670-678.

573 26. Hogquist, K.A., et al., *T cell receptor antagonist peptides induce positive selection*. Cell, 1994.  
574 **76**(1): p. 17-27.

575 27. HJ, G., *The new stereological tools: disector, fractionator, nucleator and point sampled*  
576 *intercepts and their use in pathological research and diagnosis*. Apmis, 1988. **96**: p. 857-881.

577 28. Giguere, N., S. Burke Nanni, and L.E. Trudeau, *On Cell Loss and Selective Vulnerability of*  
578 *Neuronal Populations in Parkinson's Disease*. Front Neurol, 2018. **9**: p. 455.

579 29. Cebrian, C., et al., *MHC-I expression renders catecholaminergic neurons susceptible to T-cell-*  
580 *mediated degeneration*. Nat Commun, 2014. **5**: p. 3633.

581 30. Williams, G.P., et al., *Unaltered T cell responses to common antigens in individuals with*  
582 *Parkinson's disease*. J Neurol Sci, 2023. **444**: p. 120510.

583 31. Nguyen, M., et al., *Parkinson's genes orchestrate pyroptosis through selective trafficking of*  
584 *mtDNA to leaky lysosomes*. bioRxiv, 2023: p. 2023.09. 11.557213.

585 32. Recinto, S.J., et al., *Characterizing the diversity of enteric neurons using Dopamine Transporter*  
586 *(DAT)-Cre reporter mice*. bioRxiv, 2023: p. 2023.06. 16.545271.

587 33. Laurent, C., et al., *Hippocampal T cell infiltration promotes neuroinflammation and cognitive*  
588 *decline in a mouse model of tauopathy*. Brain, 2017. **140**(1): p. 184-200.

589 34. Chen, X., et al., *Microglia-mediated T cell infiltration drives neurodegeneration in tauopathy*.  
590 Nature, 2023. **615**(7953): p. 668-677.

591 35. Jorfi, M., et al., *Infiltrating CD8(+) T cells exacerbate Alzheimer's disease pathology in a 3D*  
592 *human neuroimmune axis model*. Nat Neurosci, 2023. **26**(9): p. 1489-1504.

593 36. Su, W., et al., *CXCR6 orchestrates brain CD8(+) T cell residency and limits mouse Alzheimer's*  
594 *disease pathology*. Nat Immunol, 2023. **24**(10): p. 1735-1747.

595 37. Narendra, D.P., et al., *PINK1 is selectively stabilized on impaired mitochondria to activate*  
596 *Parkin*. PLoS Biol, 2010. **8**(1): p. e1000298.

597 38. Geisler, S., et al., *PINK1/Parkin-mediated mitophagy is dependent on VDAC1 and p62/SQSTM1*.  
598 Nat Cell Biol, 2010. **12**(2): p. 119-31.

599 39. Kawajiri, S., et al., *PINK1 is recruited to mitochondria with parkin and associates with LC3 in*  
600 *mitophagy*. FEBS Lett, 2010. **584**(6): p. 1073-9.

601 40. Matsuda, N., et al., *PINK1 stabilized by mitochondrial depolarization recruits Parkin to*  
602 *damaged mitochondria and activates latent Parkin for mitophagy*. J Cell Biol, 2010. **189**(2): p.  
603 211-21.

604 41. Dagda, R.K., et al., *Loss of PINK1 function promotes mitophagy through effects on oxidative*  
605 *stress and mitochondrial fission*. J Biol Chem, 2009. **284**(20): p. 13843-13855.

606 42. McWilliams, T.G., et al., *Basal Mitophagy Occurs Independently of PINK1 in Mouse Tissues of*  
607 *High Metabolic Demand*. Cell Metab, 2018. **27**(2): p. 439-449 e5.

608 43. Oshima, Y., et al., *Parkin-independent mitophagy via Drp1-mediated outer membrane severing*  
609 *and inner membrane ubiquitination*. *J Cell Biol*, 2021. **220**(6).

610 44. Miyazaki, N., et al., *PINK1-dependent and Parkin-independent mitophagy is involved in*  
611 *reprogramming of glycometabolism in pancreatic cancer cells*. *Biochem Biophys Res Commun*,  
612 2022. **625**: p. 167-173.

613 45. Giguere, N., et al., *Comparative analysis of Parkinson's disease-associated genes in mice reveals*  
614 *altered survival and bioenergetics of Parkin-deficient dopamine neurons*. *J Biol Chem*, 2018.  
615 **293**(25): p. 9580-9593.

616